Brain Pathology 8: 475-486 (1998)

RESEARCH ARTICLE

Microvascular and Cellular Responses in the Optic Nerve of Rats with Acute Experimental Allergic Encephalomyelitis (EAE)

Ping Hu[1], John Pollard[2], Nicholas Hunt[3], Jude Taylor[2], and Tailoi Chan-Ling[1]

[1] Department of Anatomy and Histology, Institute for Biomedical Research, [2]Department of Medicine, and [3]Department of Pathology, University of Sydney, Sydney, NSW 2006, Australia.

The optic nerve of rats with EAE was examined at various times to determine the integrity of the blood-brain barrier (BBB) and to assess monocyte-macrophage, T cell, and microglial responses. In naive control animals, leakage of horseradish peroxidase (HRP) and the presence of cells expressing major histocompatibility complex (MHC) class II antigen were evident in the meninges of the retrobulbar optic nerve. In rats with EAE, microglia in the region of the lamina cribrosa and in the regions adjacent to the meninges became activated from day 7 to 8 postinduction (pi). HRP leakage was also evident in the region of the lamina cribrosa from day 7 to 8 pi. On day 8 pi, infiltration of inflammatory cells and Monastral blue leakage were apparent in the myelinated region of the optic nerve. The intensity of these cellular and vascular changes peaked at day 12 pi, when signs of clinical disease became manifest. Monocytes-macrophages expressing MHC class II and the ED1 antigen, together with lymphocytes expressing the αβT cell receptor, constituted the major proportion of cells associated with inflammatory lesions. Thus: (i) the inherent weakness of the BBB as well as the presence of both antigen (myelin) and MHC class II$^+$ cells in the retrobulbar optic nerve are likely susceptibility factors for the frequent involvement of this region in EAE and multiple sclerosis; and (ii) activation of microglia occurs early in the pathogenesis of experimental optic neuritis.

Corresponding Author:
Dr. Tailoi Chan-Ling, Department of Anatomy and Histology F13, University of Sydney, Sydney, NSW 2006, Australia;
Tel.: 61 2 9351 2596; Fax: 61 2 9351 6556; E-mail: tailoi@anatomy.usyd.edu.au

Introduction

Breakdown of the BBB (Guy & Rao, 1984), infiltration of inflammatory cells (Hayreh *et al*., 1981), astrocytic reactions (Cammer *et al*., 1990), and demyelination (Rao, 1981) are all associated with optic neuritis in animals with EAE. An important feature of optic neuritis in these animals is that the lesions occur at a predictable site, the retrobulbar optic nerve (Guy & Rao, 1984). This feature is also characteristic of optic neuritis in individuals with MS (Carrol, 1956). Inherent weakness of the BBB in the retrobulbar optic nerve (Tso *et al*., 1975; Chan-Ling *et al*., 1992a) has been suggested to be responsible for the development of EAE and MS lesions at this site (Guy & Rao, 1984; Rao, 1981). However, previous studies have shown that cellular infiltration takes place only in the myelinated regions of the optic nerve, not in the nonmyelinated region of the retrobulbar portion of the nerve (Hayreh *et al*., 1981; Guy & Rao, 1984; Rao, 1981).

In spite of intensive clinical and histological studies, the pathogenesis of optic neuritis is not fully understood. We have investigated the possible role of the encephalitogenic antigen, the inherent weakness of the BBB, activation of microglia and expression of MHC class II antigens in the pathogenesis of experimental optic neuritis. In addition, we have carried out a quantitative analysis of the infiltration of leukocyte subsets into lesions in the optic nerve during the progression of EAE.

Materials and Methods

Experimental animals and tissue preparation. *Induction of active EAE*: Eighty (10- to 12-week-old) male JC Lewis rats were used in this study. Each rat was injected intradermally with 30 μg of purified MBP (Eylar, 1974), 0.1 ml of Freund's incomplete adjuvant (Sigma, St. Louis, MO) supplemented with 1.5 mg of H37RA *Mycobacterium tuberculosis* (Difco, Detroit, MI), and 0.1 ml of physiological saline. Animals were

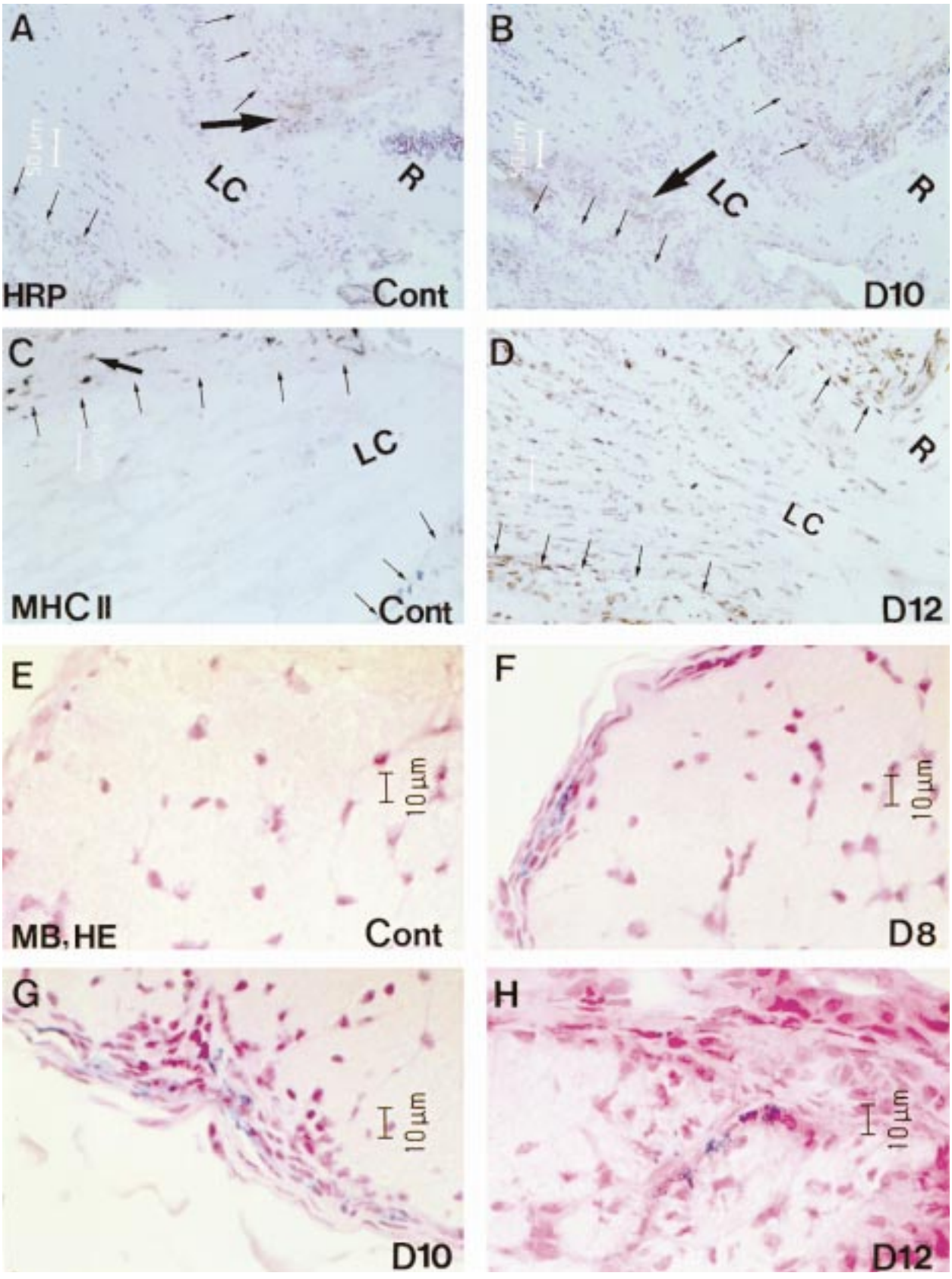
A
LC
R
HRP
Cont
B
LC
R
D10
C
LC
MHC II
Cont
D
R
LC
D12
E
10µm
MB, HE
Cont
F
10µm
D8
G
10µm
D10
H
10µm
D12

killed on days 7, 8, 10, 12, 14, 17, and 28 postinduction (pi). At each time point, three or more rats were examined by each method. Rats were examined daily for signs of EAE, and were assigned a score based on that of Juhler *et al*. (1984).

Naive and inoculated control animals: Experimental animals were compared with naive control rats as well as with animals inoculated with Freund's adjuvant containing M. tuberculosis alone; no differences in optic nerve responses were observed between the two types of control animals with the exception that more MHC class II^+ cells were observed in the meninges of inoculated controls when compared with naive controls.

Anesthesia: Rats were anesthetized for intravenous injections using 1 to 4% halothane in a 2:1 mix of nitrous oxide and oxygen. The animals were recovered from anesthesia if the intervening time between procedures exceeded 20 min. The animals were sacrificed using an intraperitoneal injection of sodium pentobarbitone (200 mg/kg).

Toluidine blue sections of optic nerve: Optic nerves were fixed by immersion in PBS containing 2.5% (v/v) glutaraldehyde and embedded in resin, sectioned at 0.25 μm, and stained with toluidine blue.

Sections of optic nerve: For ED1, TCR, CD4, CD8, and MHC class II immunohistochemistry, frozen longitudinal and transverse sections (8 μm) were postfixed in acetone at -20°C for 10 min. For staining with GS lectin, the tissue was postfixed for 4 h in 4% (w/v) paraformaldehyde in PBS, after which 50-μm-thick longitudinal sections were cut with a Lancer-1000 vibratome.

Administration of intravascular tracers. *HRP*: HRP (200 mg/kg body mass in 1 ml of physiological saline) was injected into the tail vein 20 min before the rats were killed. The optic nerve was dissected and sectioned with a cryostat and HRP was visualized (Chan-Ling *et al*., 1992b). The sections were counterstained with hematoxylin, dried in air, dehydrated in ethanol, cleared and mounted.

Monastral blue: Monastral blue is a colloidal dye, the particles of which coat, or are ingested by, activated monocytes (Neill & Hunt, 1992). It was also used to detect sites of microvascular leakage. Rats were injected in the tail vein with 1 ml of 3% (w/v) solid Monastral blue solution in 0.9% (w/v) sodium chloride (Sigma) 2 h before killing. Immediately before injection the dye was sonicated for 30 min to disrupt aggregates.

Immunohistochemistry and Histochemistry. *Detection of CD4, CD8, TCR, ED1 and MHC class II antigens*: After inactivation of endogenous peroxidase and blocking of Fc receptors by exposure to 0.1% H_2O_2 in TBS and 20% (v/v) normal calf serum in PBS for 5 min each, optic nerve sections were incubated for 45 min in a moist chamber at room temperature with the appropriate primary antibody diluted in PBS containing 1% (w/v) bovine serum albumin. The following mouse Mabs were used: rat CD4, diluted 1:100 (W3/25; MRC Cellular Immunology Unit, Oxford, UK (Williams *et al*., 1977)); rat CD8 diluted 1:25 (OX8; Cellular Immunology Unit, Oxford, UK (Mason *et al*., 1983)); rat αβTCR diluted 1:25 (R73; Cellular Immunology Unit, Oxford, UK (Hunig *et al*., 1989)); rat MHC class II (Ia) antigen diluted 1:25 (OX6; Cellular Immunology Unit, Oxford, UK (McMaster *et al*., 1979)); and ED1 diluted 1:200 (Serotec, Oxford, UK (Dijkstra *et al*., 1985)). Subsequent conjugation and visualization of sites of immunoreactivity were as previously described (Shin *et al*., 1995). Adjacent serial sections from each block were stained with hematoxylin and eosin. Staining controls, in which the primary antibody was omitted, were performed for all antibodies.

GS lectin histochemistry: Activation of monocytes and microglia results in increased staining with GS lectin (Maddox *et al*., 1982). HRP-conjugated GS lectin was used to label microglia and monocytes and the tissue was processed as previously detailed (Chan-Ling *et al*., 1990).

Quantitative cellular analysis. For quantitative analysis of monocytes-macrophages and T cell subsets in the region immediately posterior to the lamina cribrosa, serial longitudinal sections were labeled with ED1 TCR, CD4, and CD8. Two or more sections were examined for each marker for each rat. Using the 40X objective, eight fields (0.0625 mm^2) were examined in each section. T cells were considered positive and were counted if they exhibited a dense circumferential ring of

Figure 1. (Opposing page) HRP leakage (**A-B**), MHC class II antigen expression (**C-D**) and Monastral blue leakage (**E-H**) in the optic nerve of control rats and rats with EAE. Small arrows in (**A**) - (**D**) indicate meningeal surface. Retina (R). (**A**) Shows HRP leakage from meninges in the lamina cribrosa (LC) region (large arrow) of control rats. (**B**) HRP leakage with cellular infiltration (large arrow) in the parenchyma of the retrobulbar optic nerve at day 10 pi. (**C**) MHC class II^+ cells with extensive processes (large arrow) in the meninges of control rats. (**D**) EAE rat day 12 pi: Extensive expression of MHC class II in optic nerve head. (**E**) Control rat: normal optic nerve histology and no Monastral blue leakage. (**F**) Monastral blue leakage and inflammatory cells in the meninges on day 8 pi and (**G**) also in adjacent parenchyma on day 10 pi. (**H**) Monastral blue leakage and inflammatory cells in the parenchyma at day 12 pi.

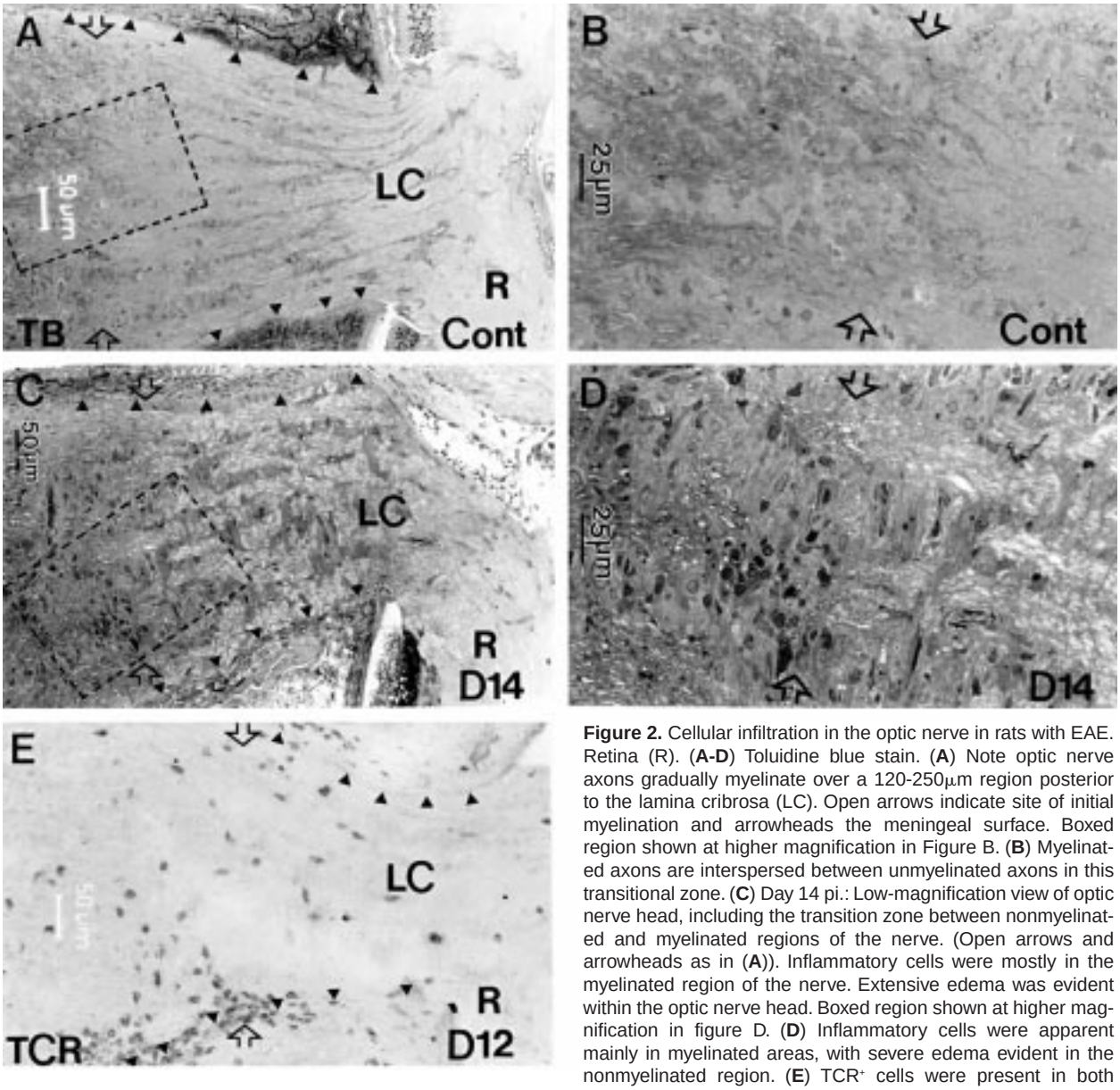

Figure 2. Cellular infiltration in the optic nerve in rats with EAE. Retina (R). (**A-D**) Toluidine blue stain. (**A**) Note optic nerve axons gradually myelinate over a 120-250µm region posterior to the lamina cribrosa (LC). Open arrows indicate site of initial myelination and arrowheads the meningeal surface. Boxed region shown at higher magnification in Figure B. (**B**) Myelinated axons are interspersed between unmyelinated axons in this transitional zone. (**C**) Day 14 pi.: Low-magnification view of optic nerve head, including the transition zone between nonmyelinated and myelinated regions of the nerve. (Open arrows and arrowheads as in (**A**)). Inflammatory cells were mostly in the myelinated region of the nerve. Extensive edema was evident within the optic nerve head. Boxed region shown at higher magnification in figure D. (**D**) Inflammatory cells were apparent mainly in myelinated areas, with severe edema evident in the nonmyelinated region. (**E**) TCR^+ cells were present in both myelinated and nonmyelinated regions on day 12 pi. (Open arrows and arrowheads as in (**A**)).

immunoreactivity. $ED1^+$ macrophages were identified mainly by their dense cytoplasmic labeling. Data were analyzed by Student's *t* test (one tailed) or chi-square test as indicated. A *P* value of <0.05 was considered statistically significant.

Results

Animal evaluation. Rats with EAE showed weight loss, ruffled fur, or altered behaviour between days 8 to 12 pi. EAE score and weight loss became statistically significant ($P < 0.05$, Student's *t* test) on day 10 pi. The maximal EAE score was achieved on days 15 to 16 pi. From day 17 pi, the rats started to recover, showing complete recovery by day 24 pi.

Inherent weakness of the BBB and existence of resident MHC class II^+ cells. HRP leakage from the meninges was apparent only in the region of the lamina cribrosa in control animals (Fig. 1A). However,

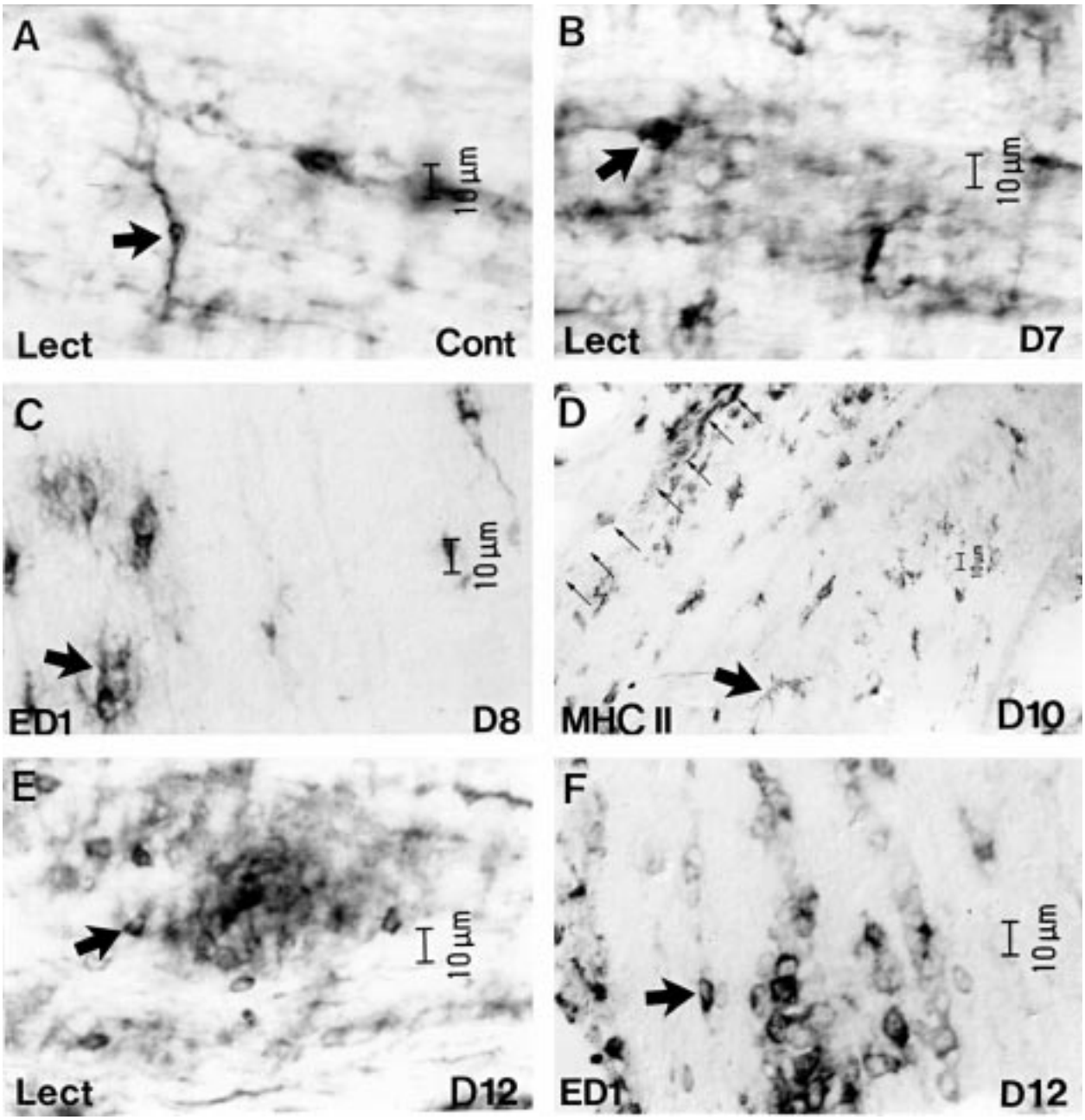

Figure 3. GS lectin$^+$, ED1$^+$ and MHC class II$^+$ cells in the optic nerve of rats with EAE. (**A**) GS lectin$^+$ (Lect) microglia in control rats showed typical ramified morphology (arrow). (**B**) Day 7 pi.: Microglial processes have become shorter and their somata larger, and the cells were stained more intensely (arrow). (**C**) Day 8 pi: The first ED1$^+$ cells detected in the parenchyma were process-bearing cells. Arrow indicates possible microglial cell. (**D**) Day 10 pi.: MHC class II$^+$ microglia (large arrow) were evident throughout the optic nerve, being most immunoreactive in the region of the lamina cribrosa (small arrows indicate meningeal surface). (**E** and **F**) Day 12 pi: most GS lectin$^+$ cells (**E**) and ED1$^+$ cells (**F**) showed monocyte-like morphology. Arrows show typical monocyte-like cells.

intravascular injection of Monastral blue revealed no evidence of leakage in the lamina cribrosa region of control animals (Fig. 1E). In both naive and inoculated control animals, a substantial population of MHC class II$^+$ cells with extensive processes (Fig. 1C) was detected in the meninges of the optic nerve.

Cellular responses and breakdown of the BBB in the optic nerve during active EAE. *First breakdown of the BBB at day 7 to 8 pi*: Traces of HRP leakage were evident from meningeal vessels and vessels within the parenchyma of the optic nerve from day 7 to 8 pi. By day 10 pi, leakage of HRP from vessels in the optic

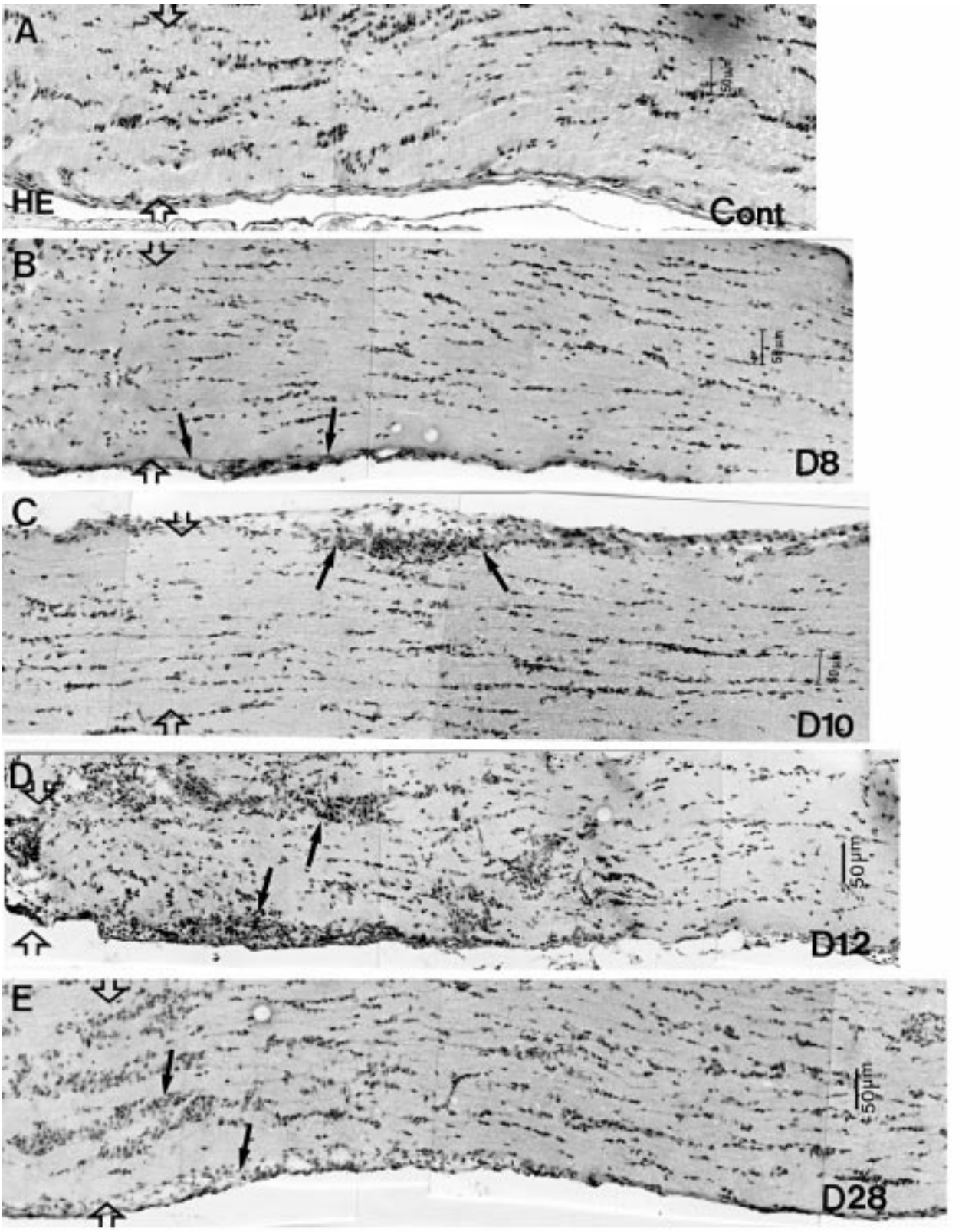
A
HE
Cont
B
D8
C
D10
D
D12
50µm
E
D28
50µm

nerve parenchyma had increased significantly (Fig 1 B). Consistent with this, edema was detected on transverse sections of optic nerve from days 10 to 14 pi (Fig. 2, C and D). Table 1 and Figure 1F-H show the time course of breakdown of the BBB using Monastral blue. Using both HRP and Monastral blue as intravascular tracers, the sites of leakage were coincident with sites of cellular infiltration.

Activation of microglia from day 7 to 8 pi: Figure 3A shows the morphology and labelling intensity with the *GS* lectin of microglia in inoculated control rat optic nerve. Activation of microglia, as indicated by increased reactivity with GS lectin (Fig. 3B), adoption of an amoeboid morphology, and expression of the ED1 antigen (Fig. 3C), was apparent from days 7 to 8 pi in the optic nerve of EAE rats. The intensity of this response increased from day 10 pi. From days 12 to 17 pi, virtually all GS lectin$^+$ (Fig. 3E) and ED1$^+$ cells (Fig. 3F) showed an amoeboid morphology.

Increased MHC class II expression within the optic nerve from day 7 to 8 pi: Compared with control animals, increased numbers of MHC class II$^+$ cells, were first evident on day 7 to 8 pi in the meninges of the optic nerve and within the parenchyma in the region of the lamina cribrosa. From this time, a small number of MHC class II$^+$ cells with a ramified morphology that resembled microglia were evident within the parenchyma of the optic nerve. The number of these cells had increased by day 10 pi (Fig. 3D). By day 12 pi, intense MHC class II expression was localized throughout the parenchyma of the optic nerve (Fig. 1D). The density of MHC class II expression was markedly higher in the myelinated region of the nerve.

Variation in the extent of cellular infiltration between myelinated and nonmyelinated regions of the optic nerve: Toluidine blue staining revealed that the transition between nonmyelinated and myelinated nerve fiber bundles in the optic nerve of control rats occurred gradually over a distance of 50 to 100 μm (Fig. 2, A and B). In EAE rats on day 12 pi, large numbers of TCR$^+$ cells were apparent predominantly in the meninges of the optic nerve but also in the parenchyma of the myelinated region of the nerve (Fig. 2E). A smaller number of TCR$^+$ cells were detected in the nonmyelinated region of the optic nerve. The region of peak cellular infiltration was coincident with the site of initial myelination in sections stained with toluidine blue from rats with EAE on day 14 pi (Fig. 2, C and D).

Time (days pi)	Leakage
(Control)	0, 0, 0, 0, 0, 0
7	0, 0, 0, 0, 0, 0
8	0, 0, 0, 1, 1, 2*
10	0, 0, 1, 1, 2, 2*
12	0, 0, 1, 1, 2, 3*
14	0, 0, 0, 0, 1, 1
17	0, 0, 0, 0, 0, 0
28	0, 0, 0, 0, 0, 0

Grades refer to individual animals: 0, no leakage; 1, low-level leakage in the meninges; 2, high-level leakage in the meninges; 3, leakage in the tissues.
*p<0.05 vs. control (chi-square test). Substantial individual variability was observed during the course of EAE.

Table 1. Subjective grading of Monastral blue leakage from optic nerve sections of JC Lewis rats during the course of acute EAE.

Hematoxylin-eosin staining revealed focal sites of cellular accumulation in the meninges of the optic nerve at the lamina cribrosa and also at the site of full myelination of optic nerve fibers by day 8 pi (Figs. 4A and B). By day 10 pi, focal sites of cellular infiltration were evident in close proximity to the meninges in the myelinated region of the optic nerve (Fig. 4C); higher magnification revealed that many leukocytes had infiltrated the parenchyma at this time (Fig. 5A). Application of cell-specific markers to serial sections showed that this cellular infiltrate consisted of ED1$^+$ (Fig. 5B), TCR$^+$ (Fig. 5C), CD4$^+$ (Fig. 5D) and CD8$^+$ (Fig. 5E) cells. The rest of the optic nerve was still predominantly free from marked cellular infiltration. By day 12 pi, cellular infiltration had spread over the entire optic nerve, being less severe at the chiasmatic end (Fig. 4D). By day 28 pi, the severity of cellular infiltration had decreased and the infiltrates were relatively evenly spread over the entire nerve (Fig. 4E); accumulation of leukocytes within the meninges was still apparent along an extensive region of the nerve.

αβTCR$^+$ lymphocyte and ED1$^+$ monocyte-macrophage infiltration from day 8 pi: Figure 6 shows a time course of accumulation of ED1$^+$ and TCR$^+$ cells in

Figure 4. (Opposing page) Development of inflammatory lesions in the optic nerve during EAE. Longitudinal sections stained with H & E. Open arrows indicate site of initial myelination. (**A**) Control rat showing normal optic nerve histology. (**B**) Inflammatory cells (solid arrows) were first evident in the submeningeal space in the retrobulbar optic nerve on day 8 pi. (**C**) Day 10 pi: focal accumulation of inflammatory cells were evident in adjoining meninges in the myelinated region (solid arrows); a higher magnification view of this region is shown in Fig. 5A. (**D**) Cellular infiltration (solid arrows) had spread throughout the nerve on day 12 pi, being less severe at the chiasmatic end. (**E**) Disseminated inflammatory cells were still evident in the parenchyma and meninges (arrows) on day 28 pi.

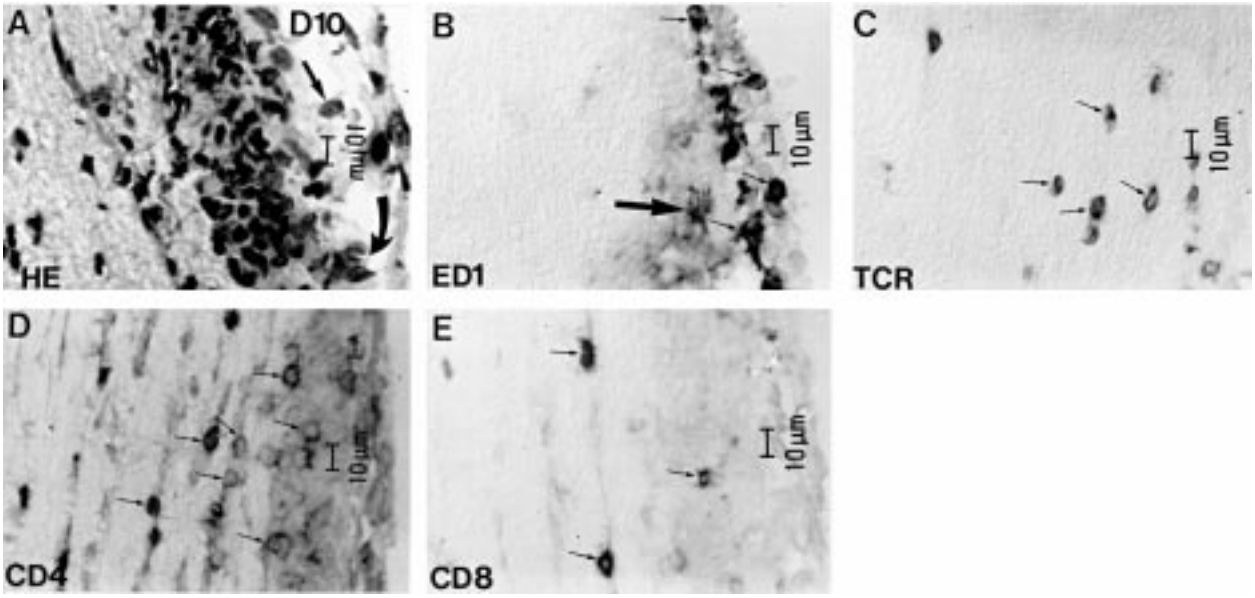

Figure 5. Leukocyte subsets on adjacent sections in optic nerve of rat with EAE, day 10 pi. Frozen sections (8 μm) of optic nerve in the region posterior to the lamina cribrosa. (**A**) Higher magnification of Fig. 4C. Cellular infiltration in the meninges and adjacent parenchyma consisted of mononuclear cells (straight arrow) and a few polymorphonuclear leukocytes (curved arrow). (**B**) ED1$^+$ cells within the meninges (small arrows) and one ED1$^+$ microglial cell within the parenchyma (large arrow). (**C** and **D**) TCR$^+$ and CD4$^+$ cells (arrows) in the region of the meninges and adjacent parenchyma. (**E**) CD8$^+$ cells (arrows) were less numerous than CD4$^+$ cells.

the parenchyma of the optic nerve during EAE. TCR$^+$ cells were first apparent at day 8 pi, peaking at day 12 and remained elevated throughout the observation period. ED1$^+$ cells first appeared at day 7 pi, increasing substantially between days 8 -10 pi. From day 8 pi, this increase in ED1$^+$ cells in the parenchyma of the optic nerve was statistically different from control animals. (P<0.05, one-tailed student's t-test). The number of ED1$^+$ cells peaked at days 12 and was significantly increased throughout the observation period. At days 12-14 pi, the density of T cells in the parenchyma was higher than the density of ED1$^+$ cells.

Predominance of CD4$^+$ cells over CD8$^+$ cells in the early stages of cellular infiltration: The first CD4$^+$ and CD8$^+$ cells were detected in the optic nerve of EAE rats on day 10 pi (Fig. 5, D and E; Fig. 6). These cells were first apparent in the meninges and in the parenchyma in close proximity to the meninges. At this early stage of cellular infiltration, the number of CD4$^+$ cells was significantly greater than the number of CD8$^+$ cells (P<0.05, one-tailed Student's t test). By day 28 pi, the density of CD8$^+$ cells was slightly greater than that of CD4$^+$ cells (Fig. 6).

Discussion

Inherent weakness of the BBB and existence of resident MHC class II$^+$ cells predisposes the optic nerve to inflammatory attack. Blood vessels in the retrobulbar optic nerve are permeable to intravascular tracers such as Evans blue and HRP (Tso *et al*., 1975; Chan-Ling *et al*., 1992a). This inherent weakness of the BBB has been suggested to be responsible for the susceptibility of this region to lesion formation in both EAE and MS (Guy & Rao, 1984). Indeed, regions of the CNS, such as spinal nerve root sheaths (Pettersson, 1993), that lack an inherent BBB often show early accumulation of inflammatory cells in animals with EAE (Shin *et al*., 1995). In addition, the periventricular white matter is susceptible to formation of plaques in individuals with MS (Adams, 1977). These observations are consistent with the hypothesis that sites of inherent breakdown of the BBB are susceptible to lesion formation in EAE and MS.

These sites of inherent weakness of the BBB are also characterized by the presence of a resident population of MHC class II$^+$ cells. In the present study we have demonstrated for the first time, the presence of a resident population of MHC class II$^+$ cells in the meninges surrounding the optic nerve and the lamina cribrosa region of the optic nerve in naive rats. These cells possess extensive processes and are possibly the equivalent

of the MHC class II$^+$ dendritic cells previously detected in the choroid plexus of the eye (Forrester *et al*., 1994). A second such site is the choroid plexus of the eye, which is not actually a part of the CNS nor does its vasculature show embryological or functional characteristics of CNS microvessels (Chan-Ling and Stone, 1993). However, because of its proximity to, and continuity with, the meninges of the optic nerve, the characteristics of the choroid are important in the development of optic neuritis. A third region of inherent leakiness is the choroid plexus within the ventricles (Brightman and Reese, 1969). We also have demonstrated the existence of a substantial population of constitutive MHC class II$^+$ cells in the region of the choroid plexus within the ventricles of naive control adult JC Lewis rats (unpublished observations). This region of the CNS is also prone to inflammatory attack during acute EAE.

The expression of MHC class II on the surface of a cell is indicative of its potential for antigen presentation (Lassmann *et al*., 1994). Expression of MHC class II is associated with the formation of inflammatory lesions in EAE (Molleston *et al*., 1993) and autoimmune diseases of the peripheral nervous system (Pollard *et al*., 1986). Therefore, the constitutive expression of MHC class II in the meninges of the retrobulbar portion of the optic nerve, observed in control rats, may contribute to the development of the inflammatory lesions in this region in rats with EAE.

Association of specific T cell subsets and macrophages with inflammatory lesions in EAE. We have characterized the temporal and spatial patterns of cellular infiltration in the optic nerve during acute EAE. Specifically, ED1$^+$ cells were first apparent in the parenchyma by day 7 pi, preceding the appearance of TCR$^+$ T cells by 1 day. ED1$^+$ and TCR$^+$ cells were first detected in the parenchyma of the retrobulbar region of the optic nerve, coincident with the sites of initial myelination and weakness of the BBB. From this location, the inflammatory cells spread within the parenchyma of the optic nerve toward the optic chiasm. T cells and monocytes-macrophages constituted the largest proportion of cells identified in inflammatory infiltrates in the optic nerve during all stages of EAE. CD4$^+$ cells were the predominant T cell subtype in the initial stages of lesion formation, although CD8$^+$ cells became the major T cell subset in the optic nerve by day 28 pi. Our observations are consistent with previous observations in the spinal cord in EAE and MS (Lassmann *et al*., 1986; Raine, 1994).

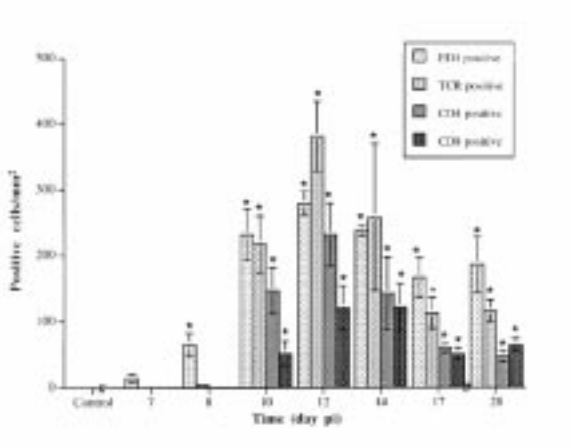

Figure 6. Quantitation of leukocyte subsets in lesions of the optic nerve in rats with EAE. Numbers of ED1$^+$, TCR$^+$, CD4$^+$, or CD8$^+$ (cells/mm^2) in the region of the optic nerve posterior to the lamina cribrosa were determined at various times pi. Data are means ± SE of 3 to 5 rats. **P*<0.05 (Student's *t* test) vs. inoculated control animals.

The role of the encephalitogenic antigen in enhancing the inflammatory cascade. Unlike optic nerve axons in humans and cats, which are fully myelinated immediately posterior to the lamina cribrosa (Blunt *et al*., 1965; Hollander *et al*., 1995), those in rats become progressively myelinated over a distance of 120 to 250 μm posterior to the lamina cribrosa (Fig. 2, A and B) (Black *et al*., 1985). Our quantitative analysis revealed that the density of infiltrating CD4$^+$, CD8$^+$, TCR$^+$, or ED1$^+$ cells increased significantly in the myelinated region of the optic nerve during the progression of acute EAE in Lewis rats. We confirmed previous studies (Hayreh *et al*., 1981; Rao, 1981) that severe cellular infiltration was evident only in the myelinated region of the optic nerve in EAE. We also detected a low-level inflammatory response in the nonmyelinated and partially myelinated regions of the optic nerve in rats with EAE. This observation is consistent with our detection of limited cellular infiltration, vascular tracer leakage, and microglial activation in the retina (see accompanying manuscript). These findings emphasise the central role of encephalolitogenic antigen (MBP) in initiating a full blown inflammatory cascade in the rat optic nerve during acute EAE.

Pathogenesis of experimental optic neuritis. Acute EAE in JC Lewis rats is an appropriate model for the early, inflammatory phase of the generation of MS plaques (Lassmann, 1983; Wekerle, 1994; Raine, 1994). Even in control animals, the lamina cribrosa region of

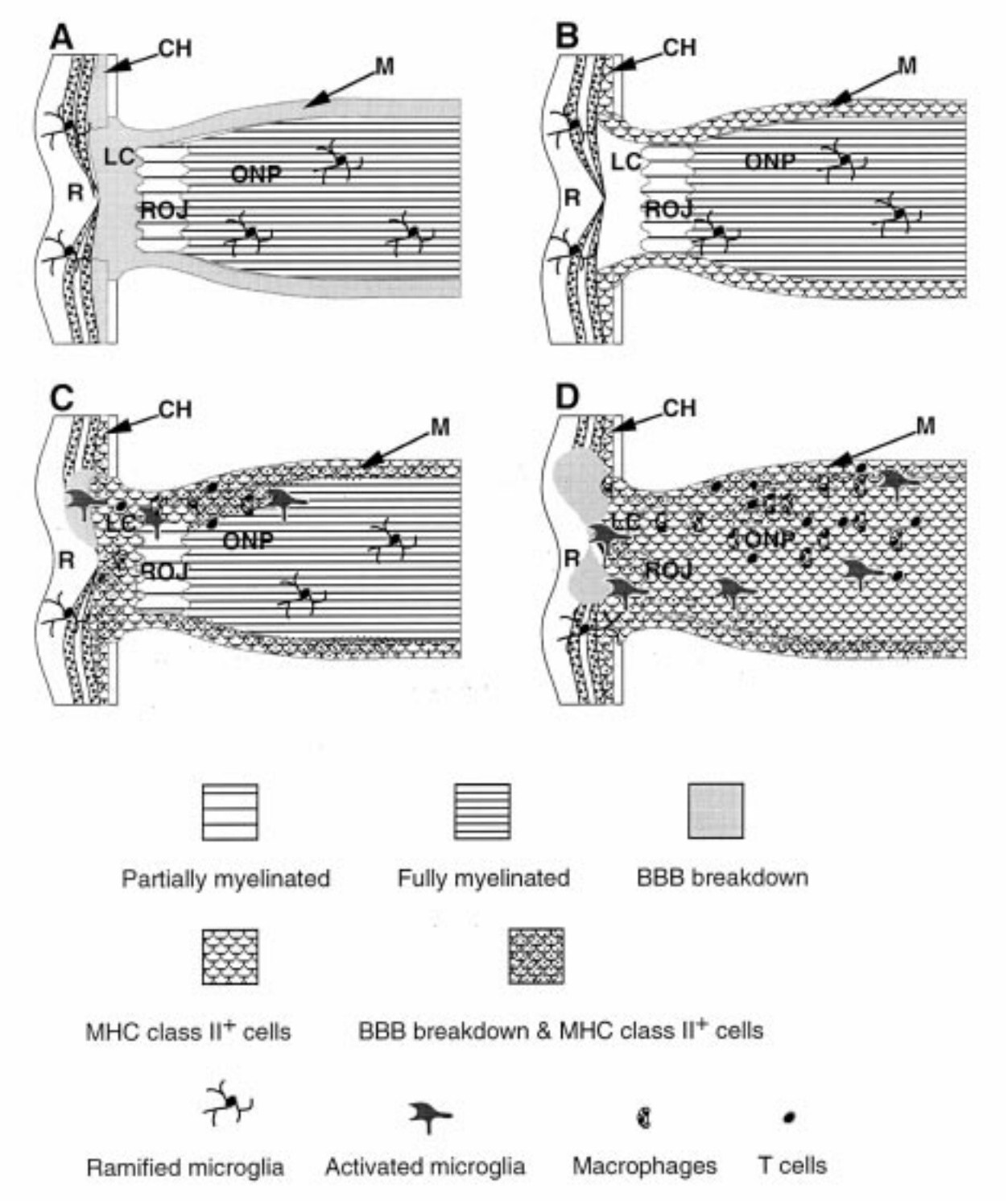
A
CH
M
LC
ONP
R
ROJ
B
CH
M
LC
ONP
R
ROJ
C
CH
M
LC
ONP
R
ROJ
D
CH
M
LC
ONP
R
ROJ
Partially myelinated
Fully myelinated
BBB breakdown
MHC class II+ cells
BBB breakdown & MHC class II+ cells
Ramified microglia
Activated microglia
Macrophages
T cells

the optic nerve and the meninges of the optic nerve are characterised by an inherent weakness of the BBB and the presence of cells expressing MHC class II antigen (Figure 7). During the early stages of acute EAE, MHC class II^+ cells, breakdown of the BBB and microglial activation are evident first in the meninges and in the lamina cribrosa region of the optic nerve. The site of initial lesion formation coincided with the site of inherent BBB breakdown and constitutive MHC class II^+ cells and microglial activation, rather than the site of initial myelination. During the peak of clinical disease, significant extravasation of mononuclear cells was evident predominantly in the myelinated region of the optic nerve, with large numbers of $CD4^+$, $CD8^+$ lymphocytes and $ED1^+$ monocytes/macrophages found in perivascular focal lesions distributed throughout the parenchyma. This marked expansion of the inflammatory cascade was only evident in the myelinated region of the optic nerve and weakened in extent towards the chiasmal end of the nerve. Our observations suggest that a combination of factors lead to the susceptibility of the optic nerve to inflammatory attack. These include the inherent weakness of the BBB, the presence of a constitutive population of MHC class II^+ cells and the amount of encephalolitogenic antigen encountered.

Acknowledgements

We thank B. Hall and J. Sedgwick for antibodies R73, OX6, W3/25, and OX8; C. Jeffrey and R. Smith for assistance with photography; and P. Kent for technical assistance.

This work was supported by grants to T.C.-L and J.P. from the National Multiple Sclerosis Society of Australia and the National Health and Medical Research Council of Australia.

References

1. Adams, CW (1977) Pathology of multiple sclerosis: progression of the lesion. *Br Med Bull* 33:15-20
2. Black JA, Waxman SG, Hildebrand C (1985) Axo-glial relations in the retina-optic nerve junction of the adult rat: freeze-fracture observations on axon membrane structure. *J Neurocytol* 14:887-907
3. Blunt MJ, Wendell-Smith CP, Baldwin F (1965) Glia-nerve fiber relationships in mammalian optic nerve. *J Anat* 99:1-11
4. Brightman MW, Reese TS (1969) Junctions between intimately opposed cell membranes in the vertebrate brain. *J Cell Biol* 40:648-677
5. Cammer W, Tansey FA, Brosnan CF (1990) Reactive gliosis in the brains of Lewis rats with experimental allergic encephalomyelitis. *J Neuroimmunol* 27:111-120
6. Carrol FD (1956) Diseases of the optic nerve. *Trans Am Acad Ophthalmol* 60:7-98
7. Chan-Ling T, Halasz, P, Stone J (1990) Development of retinal vasculature in the cat: stages, topography and mechanisms. *Curr Eye Res* 9:459-478
8. Chan-Ling T, Neill AL, Hunt NH (1992a) Early microvascular changes in murine cerebral malaria detected in retina wholemounts. *Am J Pathol* 140:1121-1130
9. Chan-Ling T, Stone J (1993) Retinopathy of prematurity in the architecture of the retina *Prog Retinal Eye Res* 12: 155-177
10. Chan-Ling T, Tout S, Hollander H, Stone J (1992b) Vascular changes and their mechanisms in the feline model of retinopathy of prematurity. *Invest Ophthalmol Vis Sci* 33:2128-2147.
11. Dijkstra CD, Dopp EA, Joling P, Kraal G (1985) The heterogeneity of mononuclear phagocytes in lymphoid organs: distinct macrophage subpopulations in the rat recognized by monoclonal antibodies ED1, ED2 and ED3. *Immunol* 54: 589-599
12. Eylar EH, Kniskern PJ, Jackson JJ (1974) Myelin basic proteins. *Methods Enzymol* 32: 323-341
13. Forrester JV, McMenamin PG, Holthouse I, Lumsden L, Liversidge J (1994) Localization and characterization of major histocompatibility complex class II-positive cells in the posterior segment of the eye: implication for induction of autoimmune uveoretinitis. *Invest Ophthalmol Vis Sci* 35:64-77

Figure 7. (Opposing page) Schematic representation of the pathogenesis of experimental optic neuritis. (**A** and **B**) In control animals, the lamina cribrosa (LC) region of the optic nerve, the meninges (M) of the optic nerve and the choroid are characterised by an inherent weakness of the BBB and the presence of cells expression MHC class II antigen. The retina-optic nerve junction (ROJ) is a transitional region spanning 250μm where ganglion cell axons are first myelinated. The region proximal to the ROJ,where the majority of ganglion cell axons are myelinated is called the optic nerve proper (ONP). Microglia in the retina (R) and optic nerve have a ramified morphology. (**C**) During the early stages of acute EAE (days 8-10 pi), MHC class II^+ cells and breakdown of the BBB is evident first in the meninges of the optic nerve and in the lamina cribrosa region of the optic nerve. Inflammatory cells at the lesions consisted predominantly of $ED1^+$ monocytes/macrophages and $CD4^+$ lymphocytes. The site of initiation of lesion formation coincided with the site of inherent BBB breakdown and MHC class II^+ cells, rather than the site of initial myelination. (**D**) During the peak of disease (days 12-14 pi), significant extravasation of mononuclear cells were evident predominantly in the ONP. This marked expansion of the inflammatory cascade was only evident in the myelinated region of the optic nerve and weakened in extent towards the chiasmal end of the nerve.

14. Guy J, Rao NA (1984) Acute and chronic experimental optic neuritis. Alteration in the blood-nerve barrier. *Arch Ophthalmol* 102:450-454.
15. Hayreh SS, Massanari RM, Yamada T, Hayreh SM (1981) Experimental allergic encephalomyelitis. I. Optic nerve and central nervous system manifestations. *Invest Ophthalmol Vis Sci* 21:256-269
16. Hollander H, Makarov F, Stefani FH, Stone J (1995) Evidence of constriction of optic nerve axons at the lamina cribrosa in normotensive eye in humans and other mammals. *Ophthalmic Res* 27:296-309
17. Hunig T, Wallny HJ, Hartley JK, Lawetzky A, Tiefenthaler G (1989) A monoclonal antibody to a constant determinant of the rat T cell antigen receptor that induces T cell activation. Differential reactivity with subsets of immature and mature T lymphocytes. *J Exp Med* 169: 73-86
18. Juhler M, Barry DI, Offner H, Konat G, Klinken L, Paulson OB (1984) Blood-brain and blood-spinal cord barrier permeability during the course of experimental allergic encephalomyelitis in the rat. *Brain Res* 302: 347-355
19. Lassmann H (1983) Comparative neuropathology of chronic experimental allergic encephalomyelitis and multiple sclerosis. New York: Springer.
20. Lassmann H, Rinner W, Hickey WF (1994) Differential role of hematogenous macrophages, resident microglia and astrocytes in antigen presentation and tissue damage during autoimmune encephalomyelitis. *Neuropathol Appl Neurobiol* 20:195-196
21. Lassmann H, Vass K, Brunner C, Seitelberger F (1986) Characterization of inflammatory infiltrates in experimental allergic encephalomyelitis. *Prog Neuropathol* 6:33-61
22. Maddox DE, Shibata S, Goldstein IJ (1982) Stimulated macrophages express a new glycoprotein receptor reactive with Griffonia simplicifolia I-B4 isolectin. *Proc Natl Acad Sci USA* 79: 166-170
23. Mason DW, Arthur RP, Dallman MJ, Green JR, Spickett GP, Thomas ML (1983) Functions of rat T-lymphocytes subsets isolated by means of monoclonal antibodies. *Immunol* 74: 57-82
24. McMaster WR., Williams AF (1979) Identification of Ia glycoproteins in rat thymus and purification from rat spleen. *Eur J Immunol* 9: 426-33
25. Molleston MC, Thomas ML, Hickey WF (1993) Novel major histocompatibility complex expression by microglia and site-specific experimental allergic encephalomyelitis lesions in the rat central nervous system after optic nerve transection. *Adv Neurol* 59:337-348
26. Neill AL, Hunt NH (1992) Pathology of fatal and resolving murine cerebral malaria. *Parasitology* 105:165-175
27. Pettersson CA (1993) Sheaths of the spinal nerve roots. Permeability and structural characteristics of dorsal and ventral spinal nerve roots of the rat. *Acta Neuropathol* 85:129-137
28. Pollard JD, McCombe PA, Baverstock J, Gatenby PA, McLeod JG (1986) Class II antigen expression and T lymphocyte subsets in chronic inflammatory demyelinating polyneuropathy. *J Neuroimmunol* 13:123-134
29. Raine CS (1994) The Dale E. McFarlin memorial lecture: immunology in the multiple sclerosis lesion. *Ann Neurol* 36: S61-71
30. Rao NA (1981) Chronic experimental allergic optic neuritis. *Invest Ophthalmol Vis Sci* 20:159-172
31. Shin T, Kojima T, Tanuma N, Ishihara Y, Matsumoto Y (1995) The subarachnoid space as a site for precursor T cell proliferation. *J Neuroimmunol* 56:171-8
32. Tso MO, Shih CY, McLean IW (1975) Is there a blood-brain barrier at the optic nerve head? *Arch Ophthalmol* 93: 815-825
33. Wekerle H, Kojima K, Lannes VJ, Lassmann H, Linington C (1994) Animal models. *Ann Neurol* 36:S47-53
34. Williams AF, Galfre G, Milstein C (1977) Analysis of cell surface xenogenic myeloma-hybrid antibodies: differentiation antigens of rat lymphocytes. *Cell* 12: 663-673